Preferred citation: C.T.J. Dodson and W.W. Sampson. Structural invariance of stochastic fibrous networks. In **Advances in Pulp and Paper Research, Oxford 2009**, *Trans. of the XIVth Fund. Res. Symp. Oxford, 2009*, (S.J. I'Anson, ed.), pp 665–691, FRC, Manchester, 2018. DOI: 10.15376/frc.2009.2.665.

STRUCTURAL INVARIANCE OF STOCHASTIC FIBROUS NETWORKS

C.T.J. Dodson[1] and W.W. Sampson[2]

[1]School of Mathematics,
[2]School of Materials, University of Manchester, PO Box 88,
Manchester, M60 1QD, UK.

May 18, 2009

ABSTRACT

We use simulation and analytic modelling to probe the structural similarity reported in the literature for fibre networks with manifestly different degrees of uniformity. From simulations of point processes in the plane to represent random, clustered and disperse fibre centres, we show that the distribution of distances between pairs of centres is very insensitive to the extent of clustering. Further, we quantify the correlation between the lengths of adjacent polygon sides arising from a Poisson line process in the plane as being $\rho = 0.616 \pm 0.001$ and show that this is very insensitive to fibre orientation and only weakly influenced by clustering. The relevance of this correlation to pore geometry is discussed.

In the final part we analyze simulated areal density maps and show that their variance relative to that of a random fibre network of the same constituent fibres, as quantified by the formation number, depends at small scales on the flocculation intensity only and depends at large scales on the number of fibres per floc only.

INTRODUCTION

At the preceding symposium, we presented an analysis of the influence on the pore size distribution of correlation between adjacent free-fibre lengths in thin networks in random (*i.e.* Poisson), flocculated, and oriented fibre networks [1], *cf.* also [2]. We conjectured that there was an intrinsic 'ground-state' positive correlation between the lengths of the adjacent free-fibre-lengths that form the perimeters of polygonal voids. This correlation explains the earlier observation that polygons (pores) in thin fibre networks tend to be 'roundish' rather than 'slit-shaped' [3]. We made the qualitative observation that the influence of fibre orientation on correlation, and hence polygon shape, was overwhelmed by the inherent random variation of density in the network. Our numerical analysis suggested also that flocculation (fibre clumping or clustering) had only a weak influence on statistics characterizing the pore size distribution.

The variance of local areal density (grammage) is known analytically for the special case of isotropic random fibre networks [4]. The ratio of variances obtained by dividing the measured β-radiographic variance of local areal density by that calculated for the same fibres in an isotropic random network yields a dimensionless statistic called the *formation number*, n_f. For commercial paper samples n_f is typically greater than 1 at scales of inspection above about 200 μm. While recognising the importance of chemical additives to the flocculation propensity of fibre suspensions, we note the result of Chatterjee [5] who studied the effects of chemical flocculants and increased suspension consistency, *i.e.* increased potential for mechanical flocculation, on formation. Chatterjee concluded that these influences were not easily distinguished, so it seems that chemical and mechanically induced interaction of fibres in suspension generate a similar class of flocculated structures.

In the context of the current study, an important result is that a plot of n_f against the scale of inspection is roughly linear up to inspection zone sizes of about 4 mm [6]; this persists for a large range of papers formed using Fourdrinier and twin-wire forming sections [7]. This indicates a similarity in structures for different paper samples and supporting evidence for this is provided by Farnood *et al.* [8], who demonstrated a strong correlation between the mean floc size and its standard deviation in machine-made papers and handsheets. Note also that although the influence of hydrodynamics in the forming section on fibre orientation tends to favour good formation [9], the direct influence of fibre orientation on formation is very weak [10, 11].

Structural stability in the distribution of mass manifests itself also in the complementary distribution of void sizes. Measurements and simulations

show that the pore radius distribution is well described by a gamma distribution [12–15] with the standard deviation of pore radii being proportional to the mean for changes in fibre morphology and flocculation [3, 15, 16]. A significant contribution to this invariance is the insensitivity of the z-directional pore structure to changes in areal density distribution (formation) [17], the dimensions of the pore height distribution dominating measurements of pores in paper [18]. Although there is some evidence of a weak influence of formation on mean pore size [15, 19], the gamma distribution holds.

The analysis presented in [1] provided a basis for this study, which seeks reasons for the seemingly narrow class of structures that are realised in papermaking processes. Again, our reference structure is the isotropic Poisson random network; the Central Limit Theorem tells us that the distribution of local areal density will be approximately Gaussian (truncated to finite domain), since it is the result of a large number of independent random fibre depositions. In fact, similar distributions are found for most papers, just with larger variances when flocculation is present.

Here, we use simulation to illustrate and quantify our conjecture that the lengths of adjacent polygon sides in isotropic random line networks, which have a controlling influence on the statistics of inter-fibre voids, are correlated and show that this correlation exhibits only a weak dependence on fibre orientation and clustering. Formation depends on the location of fibre centres relative to each other and we proceed to use simulation to show that the distribution of distances between fibre centres is extremely insensitive to the degree of flocculation in the network. In the final part we describe a formation simulator that decouples the influence of cluster (floc) size and intensity. The data arising from the simulator provide insights into the relationship between the scale of inspection and the formation number, n_f, which we interpret using an approximate analytic model.

DISTANCES BETWEEN FIBRE CENTRES

The probability density of the distance between pairs of points chosen independently and at random in a square of side d is [20]

$$b(r,d) = \begin{cases} \frac{2r}{d^4}\left(\pi d^2 - 4dr + r^2\right) & \text{for } 0 \le r \le d \\ \frac{2r}{d^4}\left(4d\sqrt{r^2-d^2} - r^2 \right. & \\ \qquad \left. -d^2\left(2+\pi-4\sin^{-1}\left(\frac{d}{r}\right)\right)\right) & \text{for } d \le r \le \sqrt{2}x \\ 0 & \text{otherwise.} \end{cases} \tag{1}$$

It can be used also to describe the distribution of distances between pairs of

fibre centres in a Poisson random fibre network. We have used simulation to calculate approximately the distribution of distances between fibre centres for disperse and flocculated networks. The distribution of fibre centres for flocculated fibre networks is simulated as a compound Poisson process occurring within a unit square. Circular regions are generated with centres occurring as a Poisson point process in the plane and points are randomly distributed within these circular regions. The number of points occurring within each circular region itself has a Poisson distribution with mean determined by the diameter of the circles (*i.e.* the cluster or 'floc' size) and and an intensity factor, I_c which is a multiple of the expected number of points per unit area in the network as a whole. Each simulation generates the locations of 50 000 points and then computes the distances between one million pairs of points selected at random from these.

Some outputs of the simulation are shown in Figure 1 for the three cases of interest: disperse, random and clustered. The left column shows the locations of a random selection of 5000 points and the centre column shows fibre networks with uniform orientation and with the locations of fibre centres given by the point process. The column on the right shows histograms of the distribution of distances between pairs of points; the solid line plotted on the same axes is the probability density function of Ghosh which was derived for the random case. As expected, the results from our simulation show excellent agreement with Ghosh's theory, but importantly the distribution obtained for the disperse case is indistinguishable from that of the Poisson random case; for the compound Poisson clustered case, we observe only a weak departure from Ghosh's theory for a simple Poisson process in the region of the maximum. Note that the simulations represented in Figure 1 consider a sufficient number of points for the statistics describing the distribution of distances between pairs of fibre centres to be stable, so can be considered representative of large zones. We therefore expect this stability of the distribution to persist in the statistics that characterize formation at larger scales. This is addressed in more detail in the sequel.

CORRELATED FREE-FIBRE-LENGTHS

In our previous analysis of the pore structure of fibrous networks [1], we conjectured that there was an intrinsic 'ground-state' positive correlation between the lengths of adjacent free-fibre-lengths. Here we use simulation to quantify this correlation and to identify the influence of fibre orientation and clustering on it. There is plenty of analytic and Monte Carlo evidence that for coherent isotropic random fibre networks, polygon statistics differ little from

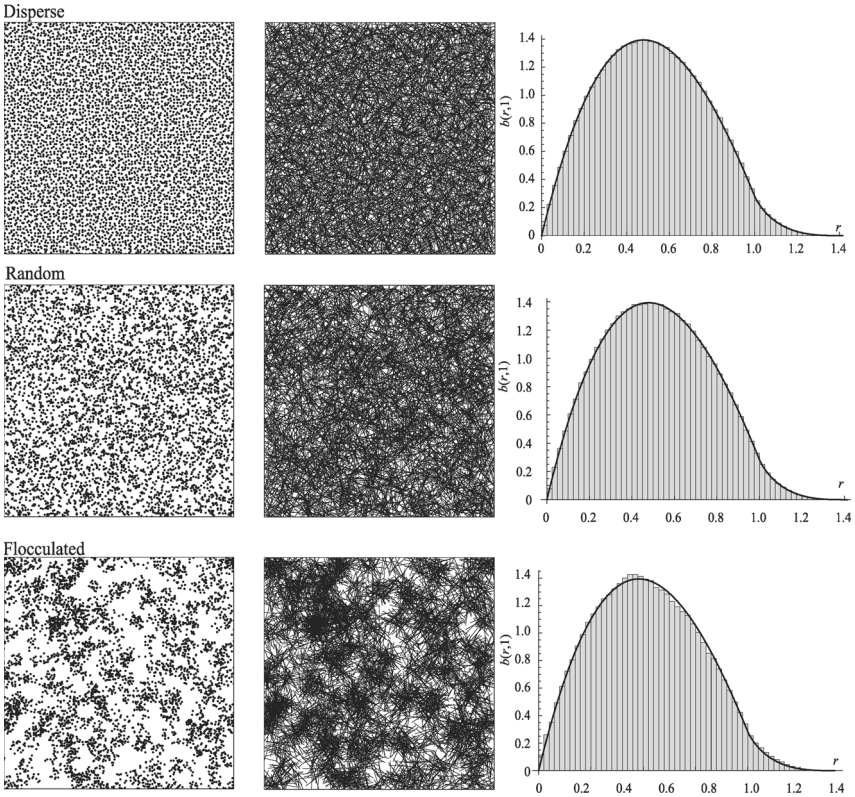

Figure 1. Left: Disperse, random and flocculated (clustered) point processes. Centre: isotropic fibre networks constructed on these with points determining fibre centres. Right: probability density function of Ghosh (lines) and histograms of spacings between centre points.

similar networks of infinite lines [21–23]. Accordingly, we consider simulations of random networks of infinite lines, thus simplifying the problem. The distribution of free-fibre-lengths in a random line network or a random fibre network is exponential [24], so before considering our simulation we derive the correlation between ordered pairs of free-fibre-lengths drawn from independent and identical exponential distributions, this provides a simple analytic reference model. The ordering of pairs is important, since without it we would necessarily have no correlation; the treatment therefore provides the effect that ordering independent random pairs has on their correlation and it takes no account of clustering of crossings. It is the latter effect that we study

by simulation: if the results of our simulation yield greater correlation, then we will have demonstrated the intrinsic 'ground state' of our earlier conjecture.

We start with pairs of randomly chosen numbers from the exponential distribution; hence the mean value of the product of these pairs is 1. Then convert each pair $\{x_i, y_i\}$ into an ordered pair (x_i, y_i) such that $x_i \leq y_i$ and create now two distributions, one for the first member x and one for the second member y. Intuitively, we take any $y_i < x_i$ from the source distribution of y and add them to source distribution of x; also we take any $x_i > y_i$ from the source distribution of x and add these to the source distribution of y. Note that the mean product of pairs $\overline{xy} = 1$ unaltered; however, the ordered pairs are no longer independent. This yields the probability density function for x:

$$g_{\leq}(x) = \frac{1}{2}\, e^{-2x} \tag{2}$$

with mean, $\bar{x} = \frac{1}{2}$ and variance, $\sigma^2(x) = \frac{1}{4}$. The probability density function for y is

$$g_{\geq}(y) = 2\, e^{-2y}(1 - e^{-y}), \tag{3}$$

with mean, $\bar{y} = \frac{3}{2}$ and variance, $\sigma^2(y) = \frac{5}{4}$.

The correlation ρ is given by

$$\begin{aligned} \rho &= \frac{\overline{x\,y} - \bar{x}\,\bar{y}}{\sigma(x)\,\sigma(y)} \\ &= \frac{1}{\sqrt{5}}. \end{aligned}$$

See also our Chapter 9 in Arwini and Dodson [2] for more discussion.

We have written *Mathematica* code to extract pairs of x and y representing the lengths of the adjacent sides of polygons arising from a Poisson line process in a unit square. The code works by solving the equations of lines drawn at random within the unit square for the coordinates of all crossings that occur between them. Each of the coordinates is identified by the lines that generate it, allowing the coordinates of the adjacent crossings on these lines to be extracted; from these the lengths of adjacent pairs of polygon sides are calculated. Graphical representations of these random line networks are shown in Figure 2. Note that we consider only pairs of polygon sides

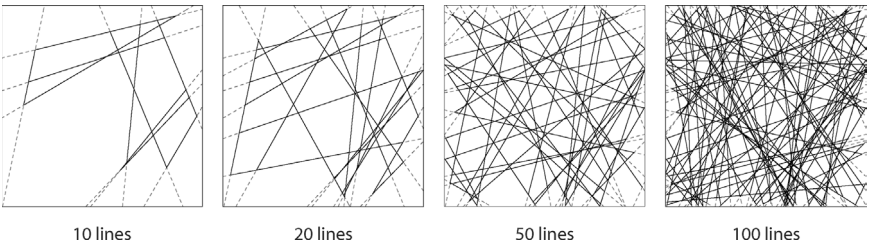

Figure 2. Graphical representation of random line processes in the plane.

bounded entirely by the unit square. Where either of a pair of adjacent polygon sides crosses the sides of the unit square, these are discounted from the analysis. In Figure 2 these polygon sides are represented by broken lines; importantly, discarding these polygon sides from our analysis had no significant influence on the distribution of polygon sides, which was exponential, as expected.

In Figure 3, the correlation between adjacent polygon side lengths is plotted against the intensity of the line process generating them. The process intensity is calculated as the total length of lines in the unit square. The error bars on ρ represent 95% confidence intervals calculated from 10 different random seed numbers. Networks with an increasing number of lines per unit area were generated each random seed, permitting the correlation to be tracked as a function of process intensity; this process is illustrated in the inset figure. For processes of 1000 lines in the unit square we calculate the correlation between more than a million pairs of adjacent polygon sides and observe a correlation of $\rho = 0.616 \pm 0.001$; this is represented by the broken horizontal line in Figure 3. We observe the same correlation in networks of 500 lines with a confidence interval varying only in the fourth decimal place. Note also that whereas the correlation for individual line processes may exceed this value at low process intensities, the mean correlation observed over our 10 cases was always less than 0.616 for process intensities less than 500. It is interesting that for processes of 20 or more lines per unit area, the correlation is always greater than that calculated for independent and ordered pairs, *i.e.* $\rho = \dfrac{1}{\sqrt{5}} \approx 0.447$ and increases rapidly towards its stable value with increasing intensity.

Now, free-fibre-lengths represent the sides of polygonal voids in the plane of the sheet. Our numerical analysis of the influence of fibre orientation and clustering on these voids suggested that these had only a weak influence on

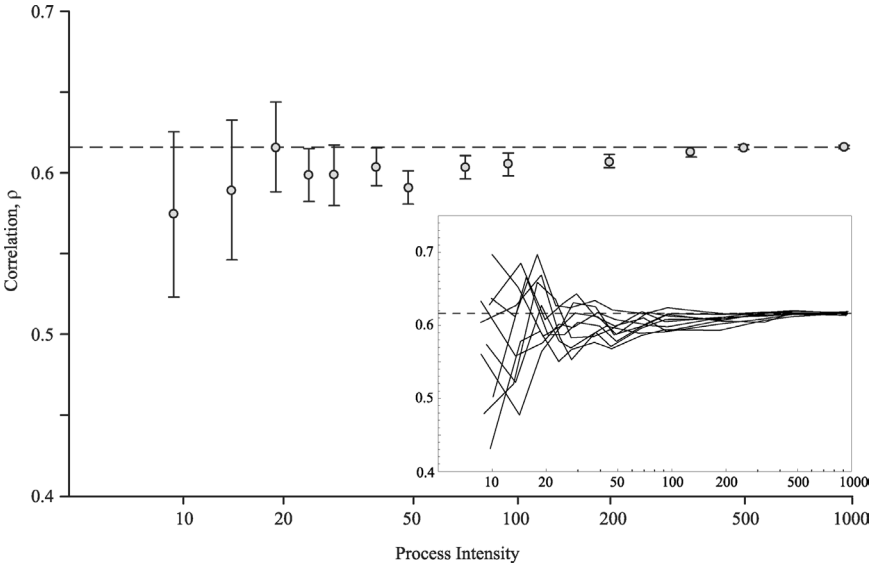

Figure 3. Correlation plotted against process intensity. Data represent the means of 10 simulations; error bars represent 95% confidence intervals. Inset diagram shows data for the 10 simulations.

the statistics characterizing the size of these voids. Further, we speculated that the inherent clustering of fibre centres was sufficiently strong to overwhelm any effect of orientation on correlation such that this would remain positive, resulting in polygonal voids tending to be 'roundish' rather than 'slit-shaped', consistent with the observations of Corte and coworkers [3, 25]. Note that 'slit-shaped', or oblong, voids require negative correlation. To investigate the effect of fibre orientation on the correlation between adjacent free-fiber-lengths, we ran our simulator for processes of 1000 lines in the unit square but with the orientation of lines, θ, distributed according to the one-parameter cosine distribution:

$$f(\theta) = \frac{1}{\pi} - \varepsilon \cos(2\theta) \qquad \text{for } 0 \leq \epsilon \leq \frac{1}{\pi} . \tag{4}$$

The correlations computed for these networks with orientation determined by the free parameter ε in Equation (4) is shown in Figure 4, where error bars represent 95% confidence intervals on the data. Although there is a systematic decrease in correlation with increasing orientation, the effect is extremely weak; indeed the minimum correlation observed over all our simulations was

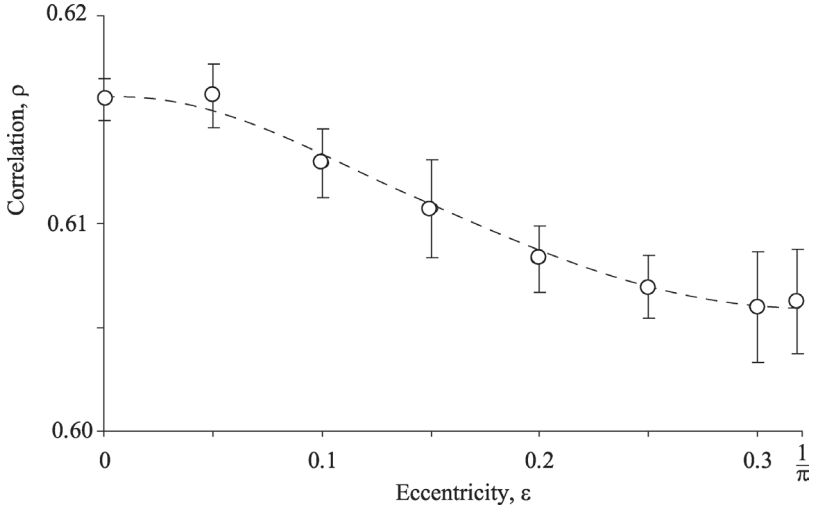

Figure 4. Correlation plotted against eccentricity for oriented networks of 1000 lines.

0.602 (when $\varepsilon = 0.3$) and the maximum was 0.619 (when $\varepsilon = 0$). Thus we have stable positive correlation for all orientations likely to be observed in a papermaking process and accordingly we expect pores to be more 'roundish' than 'slit-shaped' regardless of fibre orientation.

To identify the influence of clustering on the correlation between adjacent polygon sides, we used the simulator described earlier to generate clusters of points within circular regions of radius r_f, the number of points occurring within each circular region having a Poisson distribution with mean determined by the diameter of the circles and the intensity factor, I_c. Lines with a uniform distribution of orientations were generated to pass through these points and the correlation between adjacent sides computed. The influence of clustering is shown in Figure 5. Whereas the influence of orientation was to decrease the correlation, we now observe that clustering increases correlation and this increases with cluster radius but it is insensitive to the intensity of clustering. Importantly, although the influence of clustering on correlation is greater than that of orientation, it is not strong. Accordingly, we expect the influence of clustering on pore statistics to be correspondingly weak.

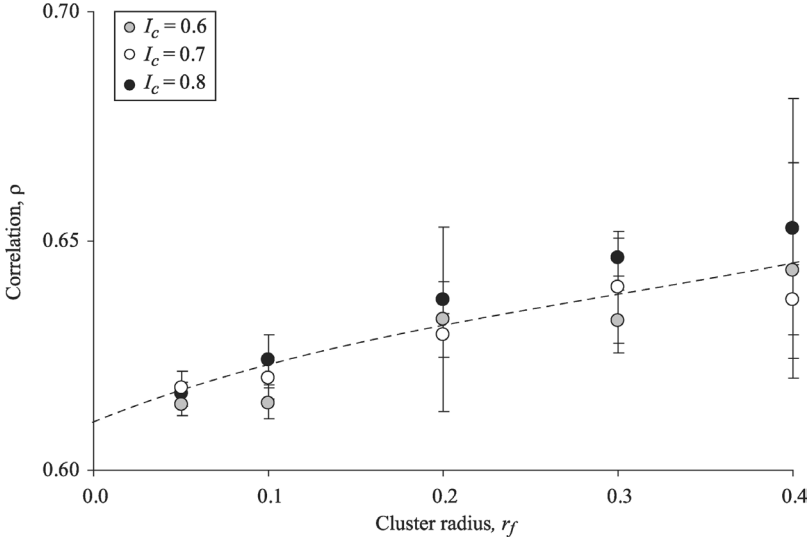

Figure 5. Correlation plotted against cluster radius for networks of 1000 lines.

FORMATION SIMULATOR

To date, no analytic model provides the variance of local grammage for flocculated structures in terms of fibre dimensions, though an approximation is provided by Farnood *et al.* who gave expressions for the distribution of mass of a Poisson process of sparse disks [8, 26]. Importantly, Farnood *et al.* found that the decay of variance of local grammage of a structure of uniform sized disks could not describe fully the behaviour observed in measurements of real samples, whereas structures of sparse disks with uniform grammage and a lognormal distribution of diameters gave excellent agreement with experimental data, though in many cases the mean disk diameters required for the model to give good agreement with experimental data were unrealistically small.

Although relationships exist between the formation number at different scales and the crowding number of the fibre suspension from which the sheet is formed [27], the hydrodynamics of sheet forming processes are sufficiently complex that variables such as jet-to-wire speed ratio, foil angles, *etc.*, will influence the size and intensity of flocculation. It is easy to characterize the resulting structures qualitatively as being 'cloudy' or 'grainy', though in a practical setting, it is difficult to isolate the influence of intensity and scale of

a flocculation process. To address this issue and to probe further the dependence of formation on the scale and intensity of fibre clustering processes, we have written a simulator that generates density maps of fibre networks where the scale and intensity of flocs may be varied independently.

Our simulator generates a 4 cm × 4 cm grammage map as an array of 400 × 400 square inspection zones, which can be considered to correspond to the pixels obtained from a calibrated scanned image of a contact β-radiograph. The code works by dropping clusters of fibres within a circular region where the centre of each cluster is distributed as a point Poisson process in the plane and the number of fibres per cluster, n_c, is a Poisson distributed random variable. The size of each cluster is determined by an intensity parameter such that the mean mass per unit area of the cluster is constant and less than the grammage of a fibre. The simulator does not incorporate the influence of fine particles or that of hydrodynamic smoothing since these will inevitably reduce the observed variability. We seek instead to quantify the scale-dependence of variability arising from a well-characterized process of fibre clustering.

The number of fibres required to generate a structure with mean grammage $\bar{\beta}$ is determined from the length, λ, and linear density (coarseness) δ of the fibres:

$$n = \frac{\bar{\beta} A}{\lambda \delta} , \tag{5}$$

where, for our simulator, $A = 16$ cm^2 and n is rounded to take an integer value.

For fibres of width ω, the grammage of a fibre is given by

$$\beta_{\text{fib}} = \frac{\delta}{\omega} . \tag{6}$$

We define a flocculation intensity $0 < I \leq 1$ such that the grammage of a cluster, corresponding to the disk grammage considered by Farnood *et al.* is given by

$$\begin{aligned} G &= I \beta_{\text{fib}} \\ &= \frac{I \delta}{\omega} . \end{aligned} \tag{7}$$

So, $0 < G \leq \beta_{\text{fib}}$. The expected number of fibres per cluster $\overline{n_c}$ is specified as an input to our simulation and the number of clusters required to form the network is computed as

$$n_{\text{cluster}} = \frac{n}{\overline{n_c}} \tag{8}$$

and rounded to the nearest integer. The code proceeds to generate a list of length n_{cluster} where each entry represents the number of fibre centres per cluster and is distributed according to a Poisson distribution with mean $\overline{n_c}$. The grammage of a cluster of radius r containing n_c fibre centres is

$$G = \frac{n_c \lambda \delta}{\pi r^2} \ . \tag{9}$$

We have assumed the grammage of a cluster to be constant and given by Equation (7), so the radius of such a cluster is given by

$$r = \sqrt{\frac{n_c \lambda \omega}{\pi I}} \tag{10}$$

We proceed to generate the coordinates of the centres of each cluster, (x,y) by selecting independent and identically distributed x and y from a uniform distribution. For each cluster we use the coordinates of the cluster centre to determine the area within which exist the n_c fibre centres associated with that cluster. These coordinates are then generated with uniform probability density within this area. Given the location of fibre centres, a uniformly distributed orientation is generated for each fibre and the coordinates of its ends are computed. For each fibre, the fraction of the fibre length that passes through each inspection zone is computed. When this has been done for every fibre, the resultant output is an array containing the total fibre length per unit area in each inspection zone; this number is multiplied by the fibre linear density to obtain the local average grammage in each zone.

Examples of density maps generated by the simulator are shown in Figure 6. We observe textures that increase in 'cloudy-ness' with n_c and increase in 'graininess' with I_c.

SCALE DEPENDENCE OF FORMATION DATA

In the Introduction, we noted that plots of the formation number, n_f against inspection zone size are approximately linear for scales of inspection less than about 4 mm. The classical approach to obtaining the variance of local grammage at different scales, from which the formation number is computed, uses complete sampling by partitioning two dimensional data into contiguous non-overlapping square inspection zones. Inevitably, as larger inspection

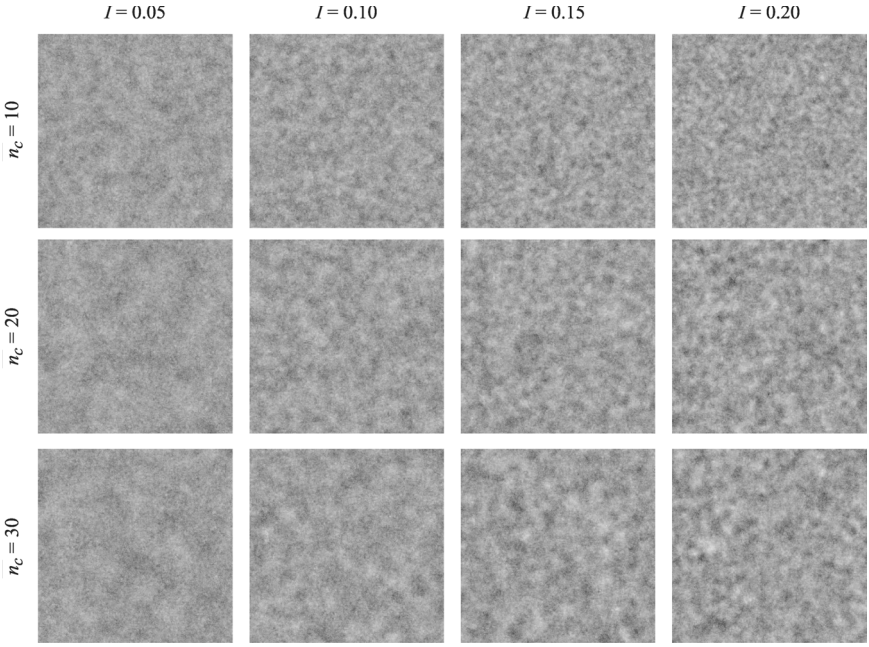

Figure 6. Simulated grammage maps each representing a 4 cm × 4 cm region with mean grammage 60 g m^{-2} formed from fibres with length $\lambda = 1$ mm, linear density $\delta = 2 \times 10^{-7}$ kg m^{-1} and width $\omega = 20$ μm.

zones are considered, the number of data available for calculation of the variance decreases.

An alternative approach is to sample the two dimensional data into overlapping square inspection zones in order that the variance may be computed for all possible arrays of contiguous square inspection zones of a given size, thus maximising the amount of data and providing a better estimate of the variance within the array at a given inspection zone size. With I'Anson, one of us has demonstrated that this approach provides the same information as the power spectrum [28], which is often used to present variance data in the frequency domain [29–31].

The use of non-overlapping inspection zones is more easily justifiable from a statistical perspective: the grammage of zones at the smallest inspection zone size is used only once to generate the distribution of local grammages at larger zone sizes. A typical grammage map obtained by calibrated contact β radiography is a square of side about 4 cm which may be scanned at a resolution of 100 μm. So at the 100 μm scale of inspection we determine the

variance of 160,000 inspection zones, at a scale of 0.4 mm we determine the variance of 10,000 inspection zones and at a scale of inspection of 4 mm we determine the variance of 100 and at a scale of 8 mm only 25 zones are available to calculate the variance. To determine the influence of the amount of available data on our calculation of the variance of local grammage, we simulated grammage maps for random fibre networks with mean grammage 60 g m^{-2} formed from fibres with linear density 2×10^{-7} kg m^{-1} and width 20 μm and varied the fibre length between 1 and 4 mm. From these simulated grammage maps we computed the variance of local grammage using non-overlapping inspection zones and overlapping inspection zones. Plots of the variance of local grammage obtained at different scales of inspection obtained using non-overlapping square zones are shown in Figure 7 and those obtained using overlapping square zones are shown in Figure 8. For each fibre length we computed also the theoretical variance of local grammage using the equations of Dodson [4]; these values are plotted as broken lines in Figures 7 and 8. For each method of partitioning the grammage map, the variance of the simulated structures agrees very well with theory for scales of inspection up to about 4 mm. As expected, sampling into non-overlapping zones results in more scatter in the observed variance as the inspection zone size increases, and hence the number of inspection zones decreases, whereas

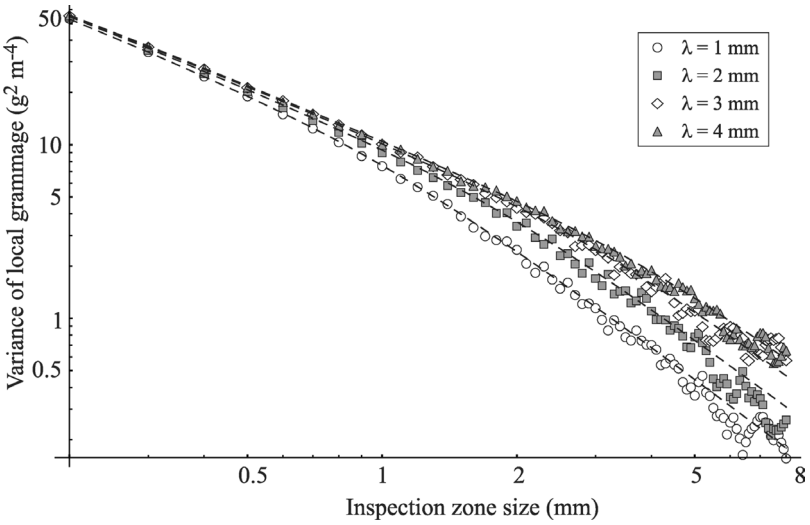

Figure 7. Variance of local grammage for non-overlapping square zones plotted against inspection zone size. Dashed lines represent theoretical variance of local grammage calculated using the theory of Dodson [4].

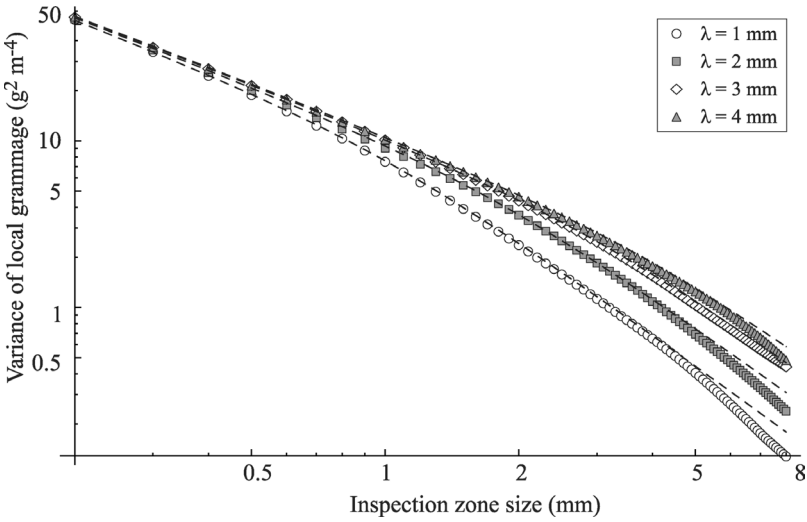

Figure 8. Variance of local grammage for overlapping square zones plotted against inspection zone size. Dashed lines represent theoretical variance of local grammage calculated using the theory of Dodson [4].

sampling by overlapping zones considerably reduces the scatter but results in an underestimation of the variance at larger zone sizes.

Dividing the calculated variance by the theoretical value obtained for a random network formed from the same fibres provides a measure of the quality of the sampling scheme. Of course, this statistic is the formation number, so for all our simulated random networks it should be very close to 1. Figures 9 and 10 show the formation number, n_f plotted against inspection zone size for non-overlapping and overlapping zones respectively. For the non-overlapping case, there is considerable scatter in the data and this increases with inspection zone size; the scatter is greatly reduced in the overlapping case, though the agreement between theory and simulation decreases at scales above 4 mm.

These results are important because they reveal that quantification of variability at large scales will always be limited by the total area of sample available for analysis. The conventional, and statistically more justifiable approach of complete sampling by contiguous non-overlapping zones provides rather a good measure of the variance at all scales, though with some scatter at larger scales. Although the absolute error is small, when the variance is divided by the theoretical variance of a random network, this can lead to very large relative errors, as evidenced by Figure 9. At scales of inspection below 4 mm,

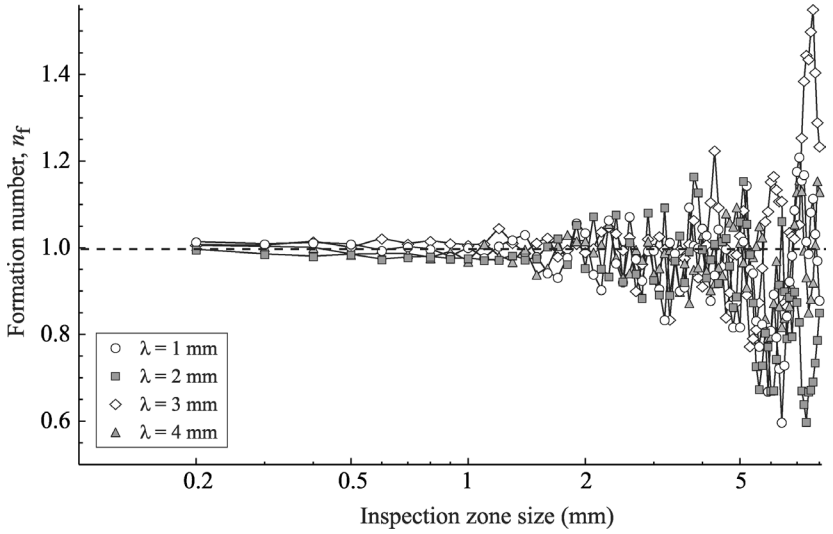

Figure 9. Formation number for non-overlapping square zones plotted against inspection zone size.

the error can be reduced by sampling with overlapping inspection zones, though at larger scales this will typically underestimate the true variance. For the simulated structures that we have considered here, 4 mm represents 10% of the sample size, so at this scale the variance is calculated for 100 inspection zones. Naturally, estimates of variance are improved as the amount of data used to compute the variance increase. This is illustrated in Figure 11 which shows the dependence of variance on sample size for three sets of random data drawn from the standard normal distribution; in each case the variance approaches that of the population from which the random numbers were drawn only when the sample size is greater than 100. In the context of analyzing paper structures, this suggests that quantitative comparison with theory, as provided by the formation number or by comparison of the power spectra with that for random networks, is only valid for scales of inspection up to 10% of the size of the sample and that above these scales we are likely to underestimate or over-estimate the formation number and this will manifest itself in spurious non-linearity of a plot of formation number against inspection zone size.

To verify this observation, we simulated a grammage map for an 8 cm × 8 cm sample formed from 2 mm fibres with the same width and linear density as used so far. The formation number of this whole region at different scales

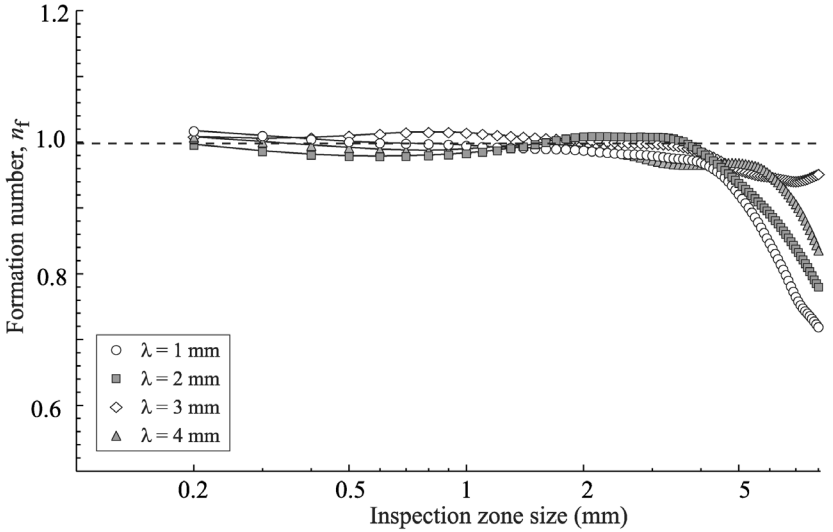

Figure 10. Formation number for overlapping square zones plotted against inspection zone size.

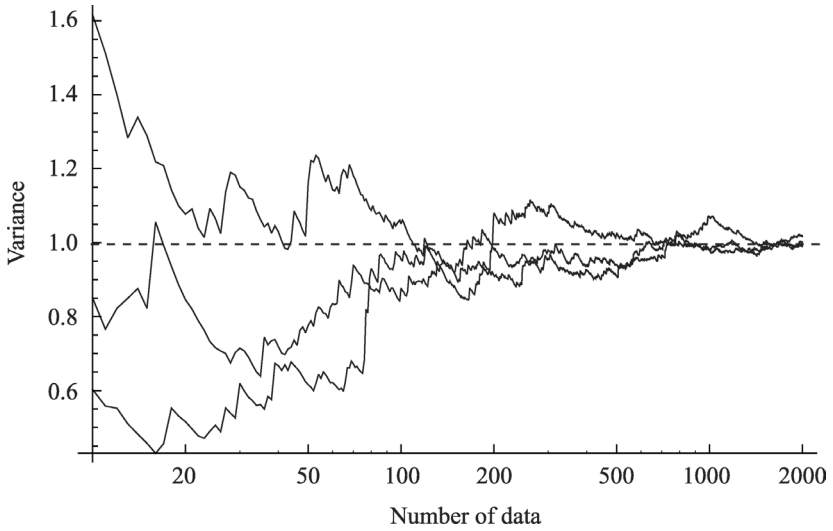

Figure 11. Dependence of variance on sample size for three sets of random data drawn from the standard normal distribution.

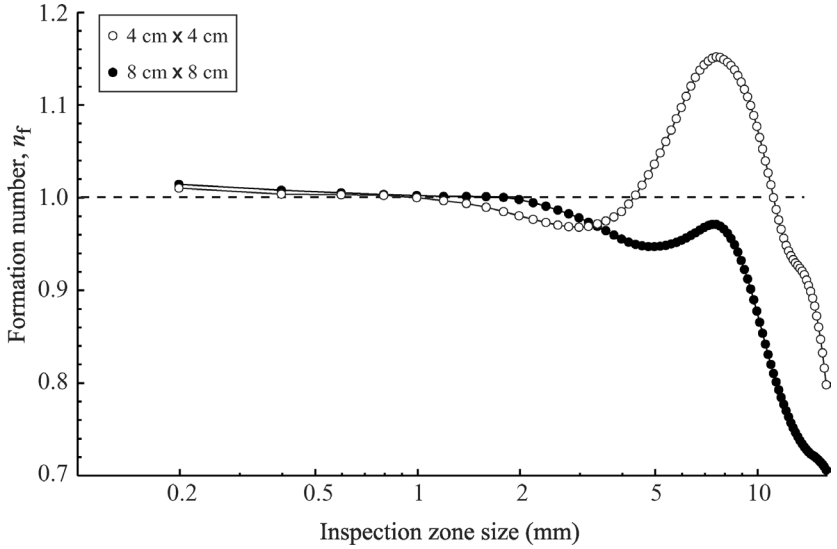

Figure 12. Influence of sample size on formation number computed for an 8 cm × 8 cm random network of 2 mm fibres with mean grammage 60 g m^{-2} and for the 4 cm × 4 cm central region.

of inspection is shown in Figure 12 along with that computed for the 4 cm × 4 cm central region. Consistent with our earlier discussion, we observe that the formation number, n_f computed for the larger sample is close to 1 for scales below about 8 mm, and for the smaller region deviation from unit value occurs at around 4 mm, so in both cases we may consider our estimate of the variance to be reliable for scales up to 10 % of the size of the sample. The result has importance for the analysis of real samples where we expect $n_f > 1$ for all but the smallest scales of inspection. We can be confident that the roughly linear relationship between n_f and inspection zone size up to scales of 4 mm or so is genuine, though the non-linearity observed at larger scales is likely to arise partly as a consequence of the limited availability of data to characterize the texture. Given the established relationship between spatial domain and frequency domain measures of formation [28], the accuracy of any measure of formation at scales more than 10% of the size of the sample is questionable. A comprehensive analysis of these effects will be reported elsewhere. For our subsequent analysis of simulated flocculated structures, we will constrain our treatment to samples of size 4 cm × 4 cm and scales of inspection up to 4 mm. Whereas larger sample areas can be generated using our simulator, the computation time for a network of given grammage

increases in proportion to sample area, so rapidly become impractical. We bear in mind also that the sample area in laboratory analyses is constrained by the size of the β-source, part of which is required for exposure of a calibration wedge.

The dependence of the formation number on zone size for simulated structures is shown in Figure 13 for networks with mean grammage 60 gm^{-2} formed from fibres with length 1 mm, linear density 2×10^{-7} kgm^{-1} and width 20 μm. Each plot represents a different flocculation intensity I and shows the influence of changing the number of fibres per cluster, n_c between 5 and 40. As expected, the formation number increases with the number of fibres per cluster and the flocculation intensity. In agreement with published data for real structures, we observe also that the formation number initially increases with inspection zone size [6, 7].

On first inspection of Figure 13 it is immediately apparent that the simulator is not yielding the linear dependence of the formation number on inspection zone size reported in the literature [6, 32]. We note however that linear regression on the data in Figure 13 yields coefficient of determination greater

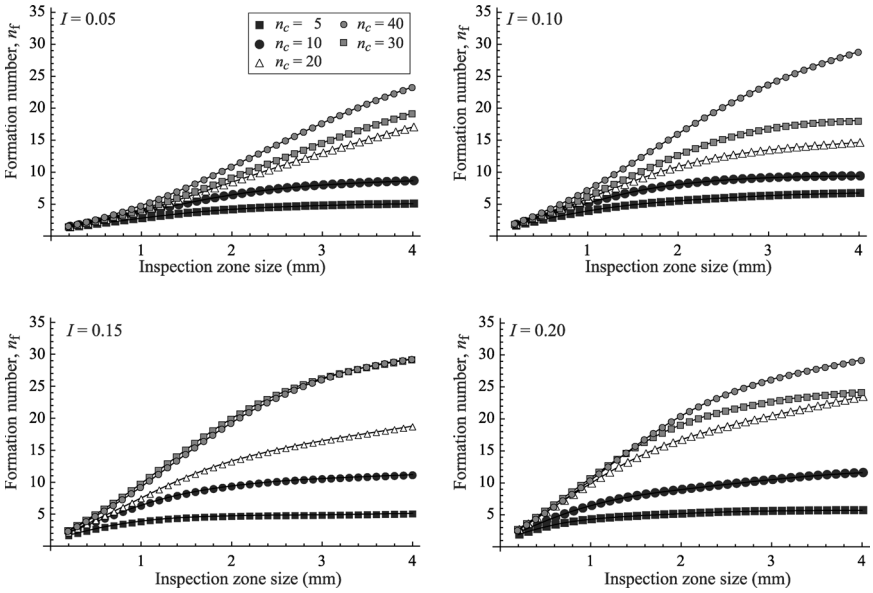

Figure 13. Influence of number of fibre centres per cluster (n_c) and flocculation intensity (I) on formation number plotted against inspection zone size for simulated structures. Mean grammage 60 g m^{-2}, λ = 1 mm, $\delta = 2 \times 10^{-7}$ kg m^{-1}, ω = 20 μm.

than 0.9 for all the curves computed for $I = 0.05$, 0.1 and for all cases except $n_c = 5$ when $I = 0.2$, so whereas curvature is readily observed, a linear approximation would characterize the scale dependency reasonably well for scales up to 4 mm. We note that the linear dependence of n_f reported in the literature [6, 7] arises from sparse data obtained at 10 or so scales of inspection only, too few to detect curvature of the type observed in Figure 13, and need not result in a low coefficient of determination for a linear regression. Similar behaviour is observed for networks of fibres with length 2 mm, as shown in Figure 14. We observe that the curve shapes in Figure 14 are similar to those at the same flocculation intensity shown in Figure 13. Although regions of some curves do scale to each other, we have been unable to identify a simple scaling law that applies over all the scales and curves plotted. One reason for this can be observed by inspection of the data obtained when

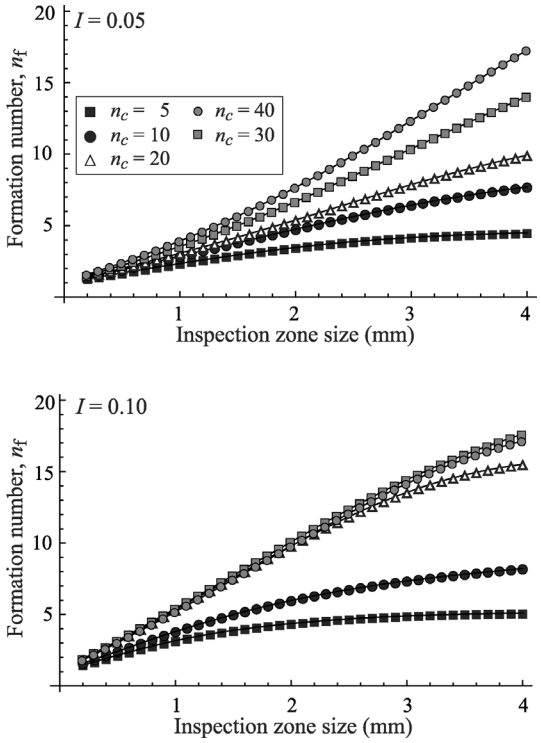

Figure 14. Influence of number of fibre centres per cluster (n_c) and flocculation intensity (I) on formation number plotted against inspection zone size for simulated structures. Mean grammage 60 g m^{-2}, $\lambda = 2$ mm, $\delta = 2 \times 10^{-7}$ kg m^{-1} $\omega = 20$ μm.

n_c = 30 and 40 for the 1 mm fibres when I = 0.2 and 0.5 and for the 2 mm fibres when I = 0.1. In these cases, the value of n_f is very insensitive to n_c over most scales such that when a large number of fibre centres are clustered within a small region, the formation number and its dependence on zone size stabilizes.

ANALYTIC APPROXIMATION

The nonlinearity in the plots of n_f against zone size shown in Figures 13 and 14 is characterized by a decreasing gradient of each curve as the inspection zone size increases, this being a stronger effect and becoming significant at smaller scales as the intensity of flocculation increases is associated with a decrease in cluster radius. We can illustrate this behaviour by considering a Poisson structure of sparse disks with uniform diameter D.

The autocorrelation function for disks with diameter D is [8]

$$\alpha_{\text{disks}}(D,r) = \frac{2}{\pi D}\left(D\,\cos^{-1}(r/D) - r\,\sqrt{1-(r/D)^2}\right) \tag{11}$$

and the variance of grammage at points of a structure with mean grammage $\bar{\beta}$ formed by the random deposition of disks with grammage G is

$$\sigma^2_{\text{disks},0}(\beta) = \bar{\beta}\,G\ . \tag{12}$$

The variance of local grammage for square zones of side x is given by

$$\sigma^2_{\text{disks,x}}(\tilde{\beta}) = \bar{\beta}\,G\int_0^{\sqrt{2}x} \alpha_{\text{disks}}(D,r)\,b(r,x)\,dr \tag{13}$$

where $b(r,x)$ is the probability density of the separation of pairs of points by a distance r as given by Equation (1). Note that here we use $b(r,x)$ to represent all possible pairs of points within a square zone, whereas earlier we used the same probability density to characterize the distribution of distances between fibre centres. Thus the integral term in Equation (13) is the fractional between zones variance of a random structure of disks with diameter D, given by the expected value of the autocorrelation function for all possible pairs of points within a square zone.

The variance of local grammage of a random fibre network is [4, 6]

$$\sigma_{\text{fibres,x}}(\tilde{\beta}) = \bar{\beta}\,\beta_{\text{fib}}\int_0^{\sqrt{2}\,x} \alpha(r,\omega,\lambda)\,b(r,x)\,dr \tag{14}$$

where $\alpha(r,\omega,\lambda)$ is the autocorrelation function for coverage at points separated by a distance r for random rectangles (fibres) with width ω and length λ.

Noting that the flocculation intensity used as a parameter in our simulations is given by $I = G/\beta_{\text{fib}}$, we obtain the formation number for our network of disks as

$$\begin{aligned} n_f(x) &= \frac{\sigma^2_{\text{disks,x}}(\tilde{\beta})}{\sigma^2_{\text{fibres,x}}(\tilde{\beta})} \\ &= I\,\frac{\int_0^{\sqrt{2}x} \alpha_{\text{disks}}(D,r)\,b(r,x)\,dr}{\int_0^{\sqrt{2}\,x} \alpha(r,\omega,\lambda)\,b(r,x)\,dr} \end{aligned} \tag{15}$$

Before tackling Equation 15 numerically, we can easily calculate analytically *for large inspection zones*

$$\lim_{x\to\infty} n_f(x) = n_c \tag{16}$$

since it is simply the ratio of variances of two Poisson processes—one for fibres and one for clusters of n_c fibres. Similarly, from the integrals we can obtain the initial slope

$$\lim_{x\to 0} \frac{dn_f(x)}{dx} = I\,\frac{\alpha_{\text{disks}}(D,r)\,b(r,x)}{\alpha(r,\omega,\lambda)\,b(r,x)}|_{r\to x\to 0} = I, \tag{17}$$

so, for Poisson networks of clumps of fibres, we know how the formation number starts and where it ends.

The influence of disk diameter on the formation number calculated for fibres of different length by numerical integration of Equation (15), is shown in Figure 15 for disks with $I = 0.1$ such that $G = \beta_{\text{fib}}/10$. On first inspection, we observe qualitative agreement with the data arising from our simulations and shown in Figures 13 and 14. Weak maxima are observed for the unrealistic cases when $\lambda > D$; for the more realistic cases with $D > \lambda$ the nonlinearity for large floc diameters is less pronounced. Some care is required in interpreting the apparent asymptotic behaviour, since the variances observed at very large scales of inspection are inevitably very small, so practical sampling schemes may exhibit a maximum in a plot of n_f against zone size with $n_f \to 1$ as $x \to \infty$.

Both our simulator and our approximate analytic model show the formation number, n_f to approach some asymptotic value depending on the scale and intensity of the fibre clusters, so at small scales the structure is closer to that of a random network than it is at large scales, *cf.* earlier discussion of distances between fibre centres. For completeness, it is illustrative to consider

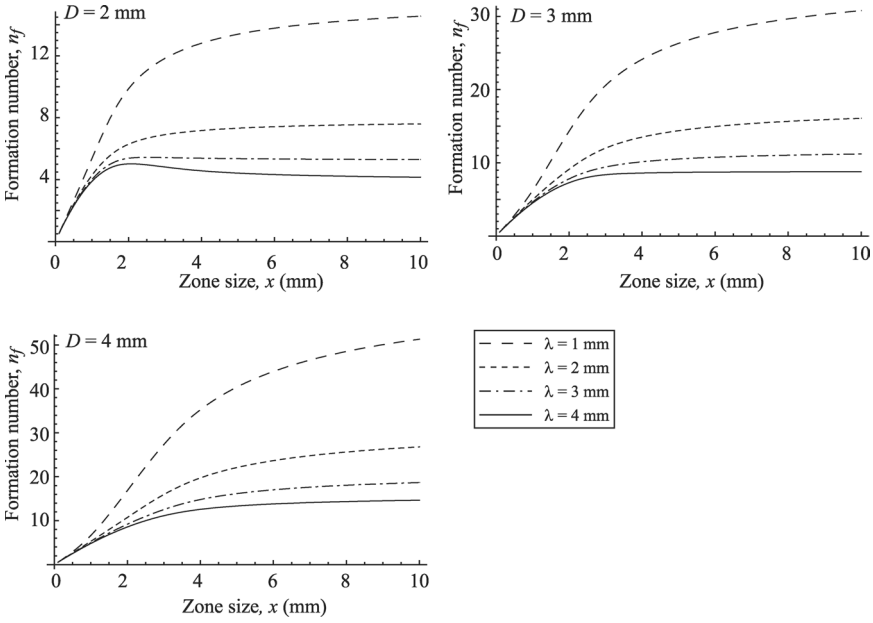

Figure 15. The formation number $n_f(x)$ for Poisson networks of clumps of fibres, from Equation (15).

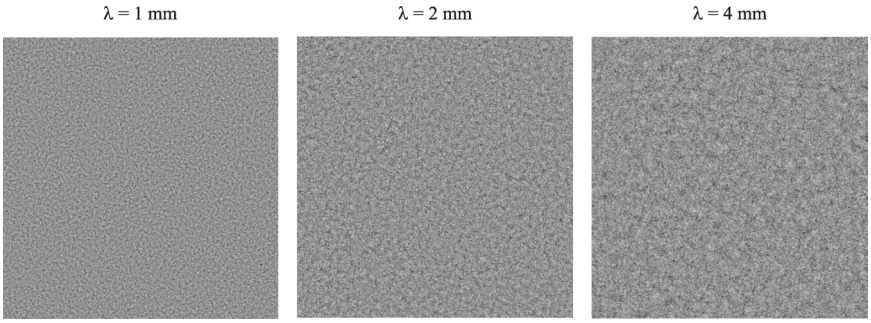

Figure 16. Grammage maps of networks of fibres with uniformly distributed orientation and with fibre centres spaced on a regular lattice.

the opposite process to clustering: a regular lattice spacing between adjacent fibre centres. Figure 16 shows 4 cm × 4 cm grammage maps generated using our simulator for regularly spaced fibre centres on a square lattice; the distribution of fibre orientations is uniform. The linear density of the fibres was

2×10^{-7} kg m^{-1}, fibre width was 20 μm and fibre lengths of 1, 2 and 4 mm were used such that the horizontal and vertical distances between fibres increased in proportion to fibre length. The formation number computed for these textures is shown in Figure 17. As anticipated, for these regular structures, the formation number is less than 1 at all scales, so they exhibit less variability than the corresponding Poisson fibre network formed from the same fibres. Importantly, the formation number for regular spacing between adjacent fibre centres is asymptotic to $n_f = 0$ as x increases, so again we have the structure at small scales being closer to that of a random network than it is at large scales, though now variability decreases with inspection zone size more rapidly in the uniform case than for random networks.

SUMMARY

We have identified two primary factors that give rise to the narrow class of structures that are realised in paper making processes:

- The distribution of distances between pairs of fibre centre points in the plane is not strongly dependent on the extent of clustering in the underlying point process.
- The correlation between the length of adjacent polygon sides arising from

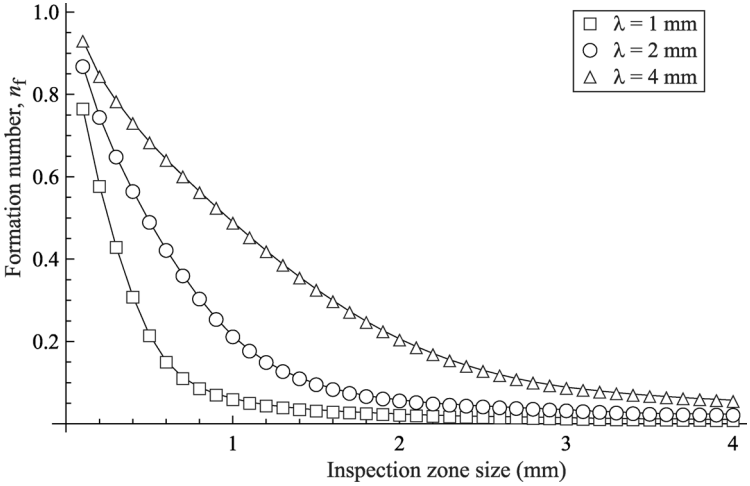

Figure 17. Formation number against inspection zone size for grammage maps shown in Figure 16.

a stochastic line process in the plane is insensitive to fibre orientation and clustering.

The latter observation has relevance to the shape of the in-plane voids in the sheet and results in these being typically 'roundish' rather that 'slit-shaped'. The first observation has relevance to the distribution of mass density. From our approximate analytic model we state that at small scales, the initial slope of a plot of formation number against zone size is given by the flocculation intensity; at large scales, the formation number is asymptotic to the expected number of fibres per floc. Our analysis of simulated textures suggests that detection of these asymptotes in practical sampling schemes is dependent on their occurrence at scales less than one tenth that of the available sample.

ACKNOWLEDGEMENT

We gratefully acknowledge the contribution of Max Sampson in repeatedly running the simulator and recording the data plotted in Figures 4 and 5.

REFERENCES

1. C.T.J. Dodson and W.W. Sampson. Effect of correlated free fibre lengths on pore size distribution in fibrous mats. In **Advances in Paper Science and Technology**. *Trans. XIIIth Fund. Res. Symp.* (S.J. I'Anson, ed.), pp 943–960, FRC, Manchester, 2005.
2. K. Arwini and C.T.J. Dodson. **Information Geometry Near Randomness and Near Independence**. Lecture Notes in Mathematics, Springer-Verlag, New York, Berlin 2008.
3. H. Corte and E.H. Lloyd. Fluid flow through paper and sheet structure. In **Consolidation of the Paper Web** *Trans. IIIrd Fund. Res. Symp.* (F. Bolam, ed.), pp 981–1009, BPBMA, London, 1966.
4. C.T.J. Dodson. Spatial variability and the theory of sampling in random fibrous networks. *J. Roy. Statist. Soc.* **B 33**(1):88–94, 1971.
5. A. Chatterjee. Physico-chemical aspects of flocculation in cellulose fibre suspensions and effects of paper formation. PhD thesis, Department of Chemical Engineering and Applied Chemistry, University of Toronto, 1995.
6. M. Deng and C.T.J. Dodson. **Paper: An Engineered Stochastic Structure**. Tappi Press, Atlanta, 1994.
7. C.T.J. Dodson, W.K. Ng and R.R. Singh. Paper Stochastic Structure Analysis Archive, University of Toronto, 1995.
8. R.R. Farnood, C.T.J. Dodson and S.R. Loewen. Modelling flocculation. Part I: Random disk model. *J. Pulp Pap. Sci.* **21**(10):J348–J356, 1995.

9. B. Norman and D. Söderberg. Overview of forming literature, 1990–2000. In **The Science of Papermaking** (C.F. Baker, ed.) *Trans. XIIth Fund. Res. Symp.* pp 431–558, FRC, Manchester, 2001.
10. C. Schaffnit and C.T.J. Dodson. A new analysis of fibre orientation effects on paper formation. *Pap. ja Puu.* **76**(5):340–346, 1994.
11. R.M. Soszyński. Simulation of two-dimensional nonrandom fibre networks. Oriented rectangles with randomly distributed centroids. *J. Pulp Pap. Sci.* **20**(4):J114–J118, 1994.
12. C.T.J. Dodson and W.W. Sampson. The effect of paper formation and grammage on its pore size distribution. *J. Pulp Pap. Sci.* **22**(5):J165–J169, 1996.
13. W.W. Sampson. Comments on the pore radius distribution in near-planar stochastic fibre networks. *J. Mater. Sci.* **36**(21):5131–5135, 2001.
14. J. Castro and M. Ostoja-Starzewski. Particle sieving in a random fiber network. *Appl. Math. Modelling* **24**(8–9):523–534, 2000.
15. C.T.J. Dodson, A.G. Handley, Y. Oba and W.W. Sampson. The pore radius distribution in paper. Part I: The effect of formation and grammage. *Appita J.* **56**(4):275–280, 2003.
16. S. Roberts and W.W. Sampson. The pore radius distribution in paper. Part II: The effect of laboratory beating. *Appita J.* **56**(4):281–283, 289, 2003.
17. C.T.J. Dodson, Y. Oba and W.W. Sampson. Bivariate normal thickness-density structure in real near-planar stochastic fibre networks. *J. Statist. Phys.* **102**(1/2):345–353, 2001.
18. W.W. Sampson and S.J. Urquhart. The contribution of out-of-plane pore dimensions to the pore size distribution of paper and stochastic fibrous materials. *J. Porous Mater.* **15**(4):411–417, 2008
19. W.W. Sampson. Unified theory for structural statistics of flocculated and random fibre networks. *J. Pulp Paper Sci.* **34**(2):91–98, 2008.
20. B. Ghosh. Random distances within a rectangle and between two rectangles. *Calcutta Math. Soc.* **43**(1):17–24, 1951.
21. H.W. Piekaar and L.A. Clarenburg. Aerosol filters–Pore size distribution in fibrous filters. *Chem. Eng. Sci.* **22**:1399–1408, 1967.
22. I.K. Crain and R.E. Miles. Monte Carlo estimates of the distributions of the random polygons determined by random lines in the plane. *J. Statist. Comput. Simul.* **4**:293–325, 1976.
23. W.W. Sampson. **Modelling Stochastic Fibrous Materials with Mathematica**. Springer-Verlag, London, 2009.
24. O. Kallmes and H. Corte. The structure of paper, I. The statistical geometry of an ideal two dimensional fiber network. *Tappi J.* **43**(9):737–752, 1960. *Errata:* **44**(6):448, 1961.
25. H. Corte. Statistical geometry of random fibre networks. In **Structure, Solid Mechanics and Engineering Design**, In proc. Southampton 1969 Civil Engineering Materials Conference, Vol. 1, (ed. M. Te'eni):pp 341–355. Wiley-Interscience, London, 1971.
26. R.R. Farnood and C.T.J. Dodson. The similarity law of formation. In proc. Tappi

1995 International Paper Physics Conference, pp 5–12, Niagara-on-the-Lake, Canada. Tappi Press, Atlanta, 1995.
27. C.T.J. Dodson. Fibre crowding, fibre contacts and fibre flocculation. *Tappi J.* **79**(9):211–216, 1996.
28. S.J. I'Anson and W.W. Sampson. Determination of spatial domain formation statistics using the Fast Fourier Transform. *Pap. ja Puu.* **85**(7):403–408, 2003.
29. B. Norman and D. Wahren. Mass distribution and sheet properties of paper. In **The Fundamental properties of Paper Related to its Uses**, *Trans. Vth Fund. Res. Symp.* (F. Bolam, ed.), pp 7–70, BPBIF, London, 1973.
30. L. Haglund, B. Norman and D. Wahren. Mass distribution in random sheets – theoretical evaluation and comparison with real sheets. *Svensk Papperstidn.* **77**(10):362–370, 1974.
31. B. Norman. The formation of paper sheets. Chapter 6 in **Paper Structure and Properties**. (J.A. Bristow and P. Kolseth, eds.), Marcel Dekker, New York, 1986.
32. R.R. Farnood. Sensing and modelling of forming and formation of paper. PhD thesis, Department of Chemical Engineering and Applied Chemistry, University of Toronto, 1995.

Transcription of Discussion

STRUCTURAL INVARIANCE OF STOCHASTIC FIBROUS NETWORKS

C.T.J. Dodson[1] and *W.W. Sampson*[2]

[1]School of Mathematics, University of Manchester, PO Box 88, Manchester, M60 1QD, UK
[2]School of Materials, University of Manchester, PO Box 88, Manchester, M60 1QD, UK

Bob Pelton McMaster University

A very nice talk, Kit. In the last talk, we heard about all those wonderful imaging technologies, which I think is going to generate enormous data files, describing the three-dimensional structure of paper. I would guess one of the real values of the kind of work you are describing is that it gives some hints as to what kind of simple numbers we could extract out of these huge data sets to characterize the three-dimensional structure of paper. Have you thought about that?

Kit Dodson

Yes, this is a fair point. We have always believed that the theoretical models provide a probe that can go where the measurements have not yet gone. So, they can provide a guide as to what would be good things to calculate. Now, we are at the situation with the 3D imaging that we were at when, 50 years ago, I started work and Derek Page was busy producing pictures of individual fibres. This was terrifying to those of us who were trying to do statistical geometry with little bits of straight lines. Now, Jean-Francis Bloch and other experimental colleagues are producing beautiful 3D images of one square millimeter. It is a challenge, what to look at, what to measure? The surface images that we saw from the movie clearly illustrated the polygonal areas bonded together, but we do know fluid gets through it!

Discussion

Jean-Claude Roux University of Grenoble.

I will try to keep to one question but I may not be able to because it was an excellent presentation. In the paper industry, and in the study of the pulp suspension analysis, we often speak of crowding factors as important parameters. Can you consider these things as well?

Kit Dodson

I am sorry, could you repeat just one more time the first question?

Jean-Claude Roux

When we analyze the pulp suspension we can characterize flocculation intensity by some factors such as the crowding factor. I was wondering if you have calculated this quantity and how can it be related to your findings? Have you been able to consider consistency?

Kit Dodson

Yes, to characterize a suspension, we have used the number of fibres in a fibre length volume as a convenient measure. I recall that, with Dick Kerekes, we did some relations between the crowding factor and formation data at different scales, and it does what you would expect. The big problem is that, as we saw from Daniel Söderberg's presentation, it is a long way from the suspension to the piece of paper that we put in the radiography machine – that is the problem and, you know, some of us are a little timid about joining the points up.

As for the consistency, well, you can see it all happening in your mixing jar. It is very hard to mix them when these guys put a lot of money into these gap-former headboxes, and look what comes out. It is very hard to separate fibres.

But one other point about the suspension; what I think has been neglected is the variability. To take up Jean-Francis Bloch's, point, it is the local variability in concentration that is fundamental, not just the average value, which is given by the crowding factor. It is the variability that is important.

Jean-Claude Roux

And I have, if you permit, a more philosophical question. How many statistical rules should you consider in order to simulate a virtual structure which is close to the real structure, according to your knowledge?

Kit Dodson

Oh no, we don't attempt to simulate the real paper. We create a set of specified, well-understood idealizations, and say that this is what we will analyze. And then we present it, and we say: we believe it bears relations to your structure because these features are universal in such structures. We do not say that we will make a copy of paper, that isn't our business. Our business is to say what the theory can tell you about the qualitative structural features, and sometimes about the quantitative ones that are not obvious.